

A note on the image system for a stokeslet in a no-slip boundary

By J. R. BLAKE

*Department of Applied Mathematics and Theoretical Physics,
University of Cambridge*

(Received 11 January 1971)

Abstract. The velocity and pressure fields for Stokes's flow due to a point force ('stokeslet') in the vicinity of a stationary plane boundary are analysed, using Fourier transforms, to obtain the image system required to satisfy the no-slip condition on the boundary. The image system, which is illustrated by diagrams, is found to consist of a stokeslet equal in magnitude but opposite in sign to the initial stokeslet, a stokes-doublet and a source-doublet, the displacement axes for the doublets being in the original direction of the force. The influence of the wall on the near and far fields is discussed. In the far field it is found that a stokeslet aligned parallel to the wall produces a stokes-doublet far-field, whereas a stokeslet normal to the wall produces a combination of a source-doublet and a stokes-quadrupole far-field. Although results can be alternatively derived by the method of Lorentz (7) using a reciprocal theorem, the present method yields much more clearly the form of the image system.

1. *Introduction.* The fundamental singular solution for a point force ('stokeslet') in an infinite viscous fluid has been known for many years, and can be extracted from the classical solution of Stokes (9) for flow past a sphere (i.e. the velocity and pressure fields). In this paper the complementary terms to the stokeslet situated at a distance from a stationary plane boundary are obtained, such that the no-slip condition can be satisfied on the plane boundary, these terms being singular at the image point.

The problem has been stated previously by Ladyzhenskaya (6) and by Cox (2), but no explicit expression for the Green's function has been given. The technique employed, Fourier transformation, is common in the theory of elasticity for this type of problem and is thoroughly explained in Sneddon's (8) book. Faxen (for numerous references see Happel and Brenner (3) section 7.4) used similar transform techniques for motion of bodies in the vicinity of walls. Other techniques for obtaining solutions, accounting for boundary wall effects, have used iterative methods (e.g. method of reflections) or alternatively have used the benefits of bispherical coordinates.

We need to construct the Greens functions $G_j^k(\mathbf{x}, \mathbf{y})$ and $H^k(\mathbf{x}, \mathbf{y})$, for the velocity and pressure fields associated with a unit point force acting in the k direction at $\mathbf{x} = \mathbf{y}$ and satisfying the no-slip condition on the plane boundary. The no-slip condition is applied only on the plane boundary (not on a body near the boundary, as we can use

a surface or line distribution of singularities in the body to satisfy the no-slip condition). Here,

$$\left. \begin{aligned} G_j^k &= u_j^k + v_j^k \\ H^k &= p^k + q^k \end{aligned} \right\} \quad (j, k = 1, 2, 3), \quad (1)$$

where u_j^k and p^k are the fundamental singular solutions for the velocity and pressure respectively. These singular solutions (u_j^k, p^k) can be obtained from the following equations of motion in an infinite viscous fluid.

$$\begin{aligned} \nabla p^k &= \mu \nabla^2 \mathbf{u}^k + \mathbf{e}^k \delta(\mathbf{x} - \mathbf{y}), \\ \nabla \cdot \mathbf{u}^k &= 0, \end{aligned} \quad (2)$$

where \mathbf{e}^k is the unit vector in the k -direction, $\delta(\mathbf{x} - \mathbf{y})$ is the Dirac delta function, μ is the viscosity, p^k the pressure and \mathbf{u}^k the velocity vector due to a point force acting in the k -direction.

This unit force gives the following velocity components,

$$u_j^k = \frac{1}{8\pi\mu} \left[\frac{\delta_{jk}}{|\mathbf{x} - \mathbf{y}|} + \frac{(x_j - y_j)(x_k - y_k)}{|\mathbf{x} - \mathbf{y}|^3} \right] \quad (3)$$

and pressure field

$$p^k = \frac{1}{4\pi} \frac{x_k - y_k}{|\mathbf{x} - \mathbf{y}|^3}, \quad (4)$$

where the modulus signs $|\mathbf{x} - \mathbf{y}|$ refer to the distance between the two points. The solutions (3) and (4) can be obtained by a three dimensional Fourier transform on the above equations (2) (see Ladyzhenskaya (6)), with suitable conditions at infinity.

The complementary terms v_j^k and q^k can be obtained for the image system and will be described in the next section. An alternative method given by Lorentz (7) used a reciprocal theorem (see Happel and Brenner (3) sections 3-4, 5) to obtain the image system. The present formulae can be shown to be equivalent to Lorentz's results, but his do not clearly yield the form of the image system. The equivalent elasticity problem for the action of a point force on a semi-infinite elastic solid glued to a rigid boundary has recently been studied by Ejike (4), although his study is limited to the axisymmetric case. These formulae will be useful in applications to slender bodies in the vicinity of plane walls. In particular, the author is currently engaged in modelling the movement of micro-organisms in the vicinity of microscope slides, and in analysing the beat of a single cilium attached to the surface of an organism.

2. Image system. We now turn to the problem of obtaining complementary solutions for the velocity and pressure field due to a stokeslet situated at \mathbf{y} , a distance h above a plane boundary S , where the no-slip condition is applied. The complementary terms v_j^k and q^k satisfy the creeping flow equations in V (see diagram).

$$\left. \begin{aligned} \nabla q^k &= \mu \nabla^2 \mathbf{v}^k, \\ \nabla \cdot \mathbf{v}^k &= 0. \end{aligned} \right\} \quad (5)$$

This set of equations implies that the pressure term q^k is harmonic, i.e.

$$\nabla^2 q^k = 0. \quad (6)$$

The above equations have the following boundary conditions

$$\mathbf{v}^k(S) = -\mathbf{u}^k(S), \quad (7)$$

where S defines the set of points on the plane boundary.

However, the analysis is considerably simplified if we take a point force of equal magnitude, but opposite sign at the image point \mathbf{y}' , where

$$\mathbf{y} - \mathbf{y}' = 2h\mathbf{m},$$

\mathbf{m} being the normal to the plane boundary S . We define $\mathbf{r} = \mathbf{x} - \mathbf{y}$, $\mathbf{R} = \mathbf{x} - \mathbf{y}'$, with components (r_1, r_2, r_3) and (R_1, R_2, R_3) in the (x_1, x_2, x_3) directions respectively. The distances will be denoted by r and R . Thus

$$\left. \begin{aligned} v_j^k &= -\frac{1}{8\pi\mu} \left[\frac{\delta_{jk}}{R} + \frac{R_j R_k}{R^3} \right] + \omega_j^k, \\ q^k &= -\frac{1}{4\pi} \frac{R_k}{R^3} + S^k. \end{aligned} \right\} \quad (8)$$

The analysis is further simplified if we take the plane boundary to be $x_3 = 0$. The following are the boundary conditions for ω_j^k

$$\omega_j^k(R_1, R_2, h) = \frac{h}{4\pi\mu} (\delta_{j3}\delta_{k\alpha} + \delta_{k3}\delta_{j\alpha}) \frac{R_\alpha}{R_0^3}, \quad (9)$$

where α assumes the values 1 or 2 and $R_0 = (R_1^2 + R_2^2 + h^2)^{1/2}$ is the distance from the point forces to a point on the plane boundary (see Diagram 1).

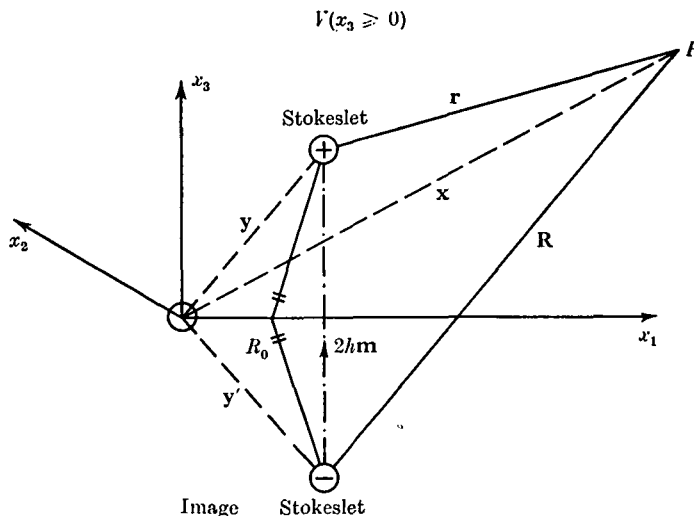


Fig. 1. The position of stokeslet and image, and relevant vectors \mathbf{x} , \mathbf{r} and \mathbf{R} .
Plane boundary $S: x_3 = 0$, $\mathbf{m} = \mathbf{i}_3$.

It can be noticed that for $k = 1$ or 2 , the tangential velocities (in (9)) on the boundary are zero, but the normal velocity is not. However for $k = 3$, the normal velocity is zero, but the tangential velocities are non zero. ω_j^k is a symmetric tensor with the 'inner' (2×2) tensor (i.e. $j, k = 1, 2$) being the null one. We thus have to obtain ω_j^k satisfying the creeping flow equations (5) and the above boundary conditions (9).

To solve these equations, the following two dimensional Fourier transform is used,

$$\hat{\phi}(\lambda_1, \lambda_2, R_3) = \frac{1}{2\pi} \iint_{-\infty}^{\infty} \phi(R_1, R_2, R_3) e^{i(\lambda_1 R_1 + \lambda_2 R_2)} dR_1 dR_2 \quad (10)$$

where $i = \sqrt{-1}$. In tensor notation the Fourier transformed equations of motion may be reduced to,

$$\left. \begin{aligned} -i\lambda_\alpha \delta_{\alpha j} \hat{s}^k + \delta_{j3} \frac{\partial \hat{s}^k}{\partial R_3} &= \mu L(\hat{\omega}_j^k), \\ -i\lambda_\alpha \hat{\omega}_\alpha^k + \frac{\partial \hat{\omega}_3^k}{\partial R_3} &= 0, \\ L(\hat{s}^k) &= 0, \end{aligned} \right\} \quad (11)$$

where

$$L = \frac{\partial^2}{\partial R_3^2} - \xi^2, \quad \xi^2 = \lambda_1^2 + \lambda_2^2$$

and the summation with respect to α is for $\alpha = 1$ and 2 .

The solution of the last equation is

$$\hat{s}^k = B^k e^{-\xi R_3} \quad (12)$$

the positive root being neglected as s^k , the pressure, tends to zero at infinity. From (12) we deduce that the representative solutions for $\hat{\omega}_j^k$ are

$$\hat{\omega}_j^k = B_j^k e^{-\xi R_3} + \frac{B^k}{2\mu} \left[\frac{i\lambda_\alpha}{\xi} \delta_{\alpha j} + \delta_{j3} \right] (R_3 - h) e^{-\xi R_3}. \quad (13)$$

The values of B_j^k can be obtained from the boundary conditions on $R_3 = h$ ($x_3 = 0$), thus $B_j^k = \hat{\omega}_j^k(R_1, R_2, h)$. The remaining term B^k is obtained from the continuity equation, thus uniquely defining the pressure field. To obtain the Fourier transformed boundary conditions on $R_3 = h$, it is more convenient to convert to Hankel transforms (Erdelyi (5)). On equating, the solutions $\hat{\omega}_j^k, \hat{s}^k$ for the Fourier transforms are,

$$\begin{aligned} \hat{\omega}_j^k &= \frac{h}{4\pi\mu} \left[\left\{ \frac{i\lambda_\alpha}{\xi} (\delta_{j3} \delta_{k\alpha} + \delta_{k3} \delta_{j\alpha}) + \left[i\lambda_\alpha (\delta_{j3} \delta_{k\alpha} - \delta_{\alpha j} \delta_{k3}) - \frac{\lambda_\alpha \lambda_\beta}{\xi} \delta_{\alpha j} \delta_{\beta k} \right. \right. \right. \\ &\quad \left. \left. \left. - \delta_{k3} \delta_{j3} \xi \right] (R_3 - h) \right\} e^{-\xi R_3} \right] \\ \hat{s}^k &= \frac{h}{2\pi} (i\lambda_\alpha \delta_{k\alpha} - \delta_{k3} \xi) e^{-\xi R_3} \end{aligned} \quad (14)$$

where β takes only the values 1 or 2 (similar to α). Equations (14) are inverted using the conjugate of equation (10).

The solution obtained for ω_j^k and s^k are,

$$\left. \begin{aligned} \omega_j^k &= \frac{h}{4\pi\mu} (\delta_{k\alpha} \delta_{\alpha l} - \delta_{k3} \delta_{l3}) \frac{\partial}{\partial R_l} \left[\frac{h R_j}{R^3} - \left(\frac{\delta_{j3}}{R} + \frac{R_j R_3}{R^3} \right) \right] \\ s^k &= -\frac{h}{2\pi} (\delta_{k\alpha} \delta_{\alpha l} - \delta_{k3} \delta_{l3}) \frac{\partial}{\partial R_l} \left(\frac{R_3}{R^3} \right). \end{aligned} \right\} \quad (15)$$

It should be emphasized that the term $(\delta_{k\alpha} \delta_{\alpha l} - \delta_{k3} \delta_{l3})$ is non-zero only if $k = l$, when it has a positive sign for $k = 1$ or 2 and negative sign for $k = 3$. Mathematically,

the variation in sign is due to the induced velocities on the plane boundary by the initial and image stokeslets, being different for the two cases. This change in sign has interesting implications which are discussed in a later section.

3. *Interpretation of results.* The entire velocity field \mathbf{u}^* and pressure field p^* for a point force F_k in the k -direction in the vicinity of the plane wall can now be written as,

$$u_j^* = \frac{F_k}{8\pi\mu} \left[\left(\frac{1}{r} - \frac{1}{R} \right) \delta_{jk} + \frac{r_j r_k}{r^3} - \frac{R_j R_k}{R^3} + 2h(\delta_{kx}\delta_{xj} - \delta_{k3}\delta_{3j}) \frac{\partial}{\partial R_i} \left(\frac{hR_j}{R^3} - \left(\frac{\delta_{j3}}{R} + \frac{R_j R_3}{R^3} \right) \right) \right] \quad (16)$$

$$p^* = \frac{F_k}{4\pi} \left[\frac{r_k}{r^3} - \frac{R_k}{R^3} - 2h(\delta_{kx}\delta_{xj} - \delta_{k3}\delta_{3j}) \frac{\partial}{\partial R_i} \left(\frac{R_3}{R^3} \right) \right],$$

where the initial point force is situated at (y_1, y_2, h) , the image at $(y_1, y_2, -h)$ and $r = [(x_1 - y_1)^2 + (x_2 - y_2)^2 + (x_3 - h)^2]^{\frac{1}{2}}$ and $R = [(x_1 - y_1)^2 + (x_2 - y_2)^2 + (x_3 + h)^2]^{\frac{1}{2}}$.

Obviously for $r \ll h$ the solution in the near field around the stokeslet is that of an isolated stokeslet in an infinite viscous fluid. However, the outer field is considerably modified by the presence of the wall. This aspect is discussed in the next section.

To help us with a description of the image system, a brief discussion of stokes-doublet is presented. Following Batchelor (1) we will define a stokes-doublet with tensorial strength D_{jk} (the definition of D_{jk} being altered slightly so that it is more appropriate for this paper) by,

$$u'_i = \frac{D_{jk}}{8\pi\mu} \left[\left\{ -\frac{r_i}{r^3} + \frac{3r_i r_j r_k}{r^5} \right\} + \left\{ \frac{r_k \delta_{ij} - r_j \delta_{ik}}{r^3} \right\} \right], \quad (17)$$

$$p' = \frac{D_{jk}}{4\pi} \left\{ \frac{3r_j r_k}{r^5} \right\},$$

where \mathbf{u}' is the velocity vector and p' the pressure associated with the stokes-doublet. This tensorial representation D_{jk} for a stokes-doublet may be interpreted as the negative value of the gradient in the k -direction of a stokeslet in the j -direction. The first set of bracketed terms in equation (17) are symmetric, whereas the second bracket is antisymmetric, which Batchelor (1) calls a stresslet and a couplet respectively. The streamlines for the stresslet are radial, whereas in the couplet they are circular. Fig. 2 is used to illustrate the decomposition of a stokeslet into a stresslet and a couplet.

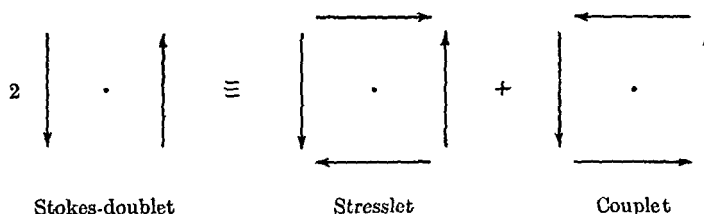


Fig. 2. A diagram representing the components of a stokes-doublet D_{jk} ($j \neq k$).

To represent the contributions to the velocity field by the stokeslet, stokes-doublet and source-doublet of the image system, the following two diagrams are used, Figs. 3 and 4. In Fig. 3, the axis of the initial stokeslet is aligned parallel to the plane boundary.

The image system in this case consists of a stokeslet of equal magnitude and opposite in sign (i.e. in x_1 or x_2 -direction), a stokes-doublet of strength $2h$ of the stokeslet and a source-doublet of strength $2h^2$ of the stokeslet. The stokes-doublet consists of equal and opposite stokeslets orientated in the normal (x_3) direction to the plane boundary, and with their displacement axis in the x_1 (or x_2) direction which in the tensorial notation is represented by D_{31} (or D_{32}). Similarly, the source-doublet has displacement axis in the x_1 -direction. The stokes-doublet in this case is of magnitude $D_{31} = 2hF_1$, which is equal in strength in the far-field to the combined influence of the initial and image stokeslets.

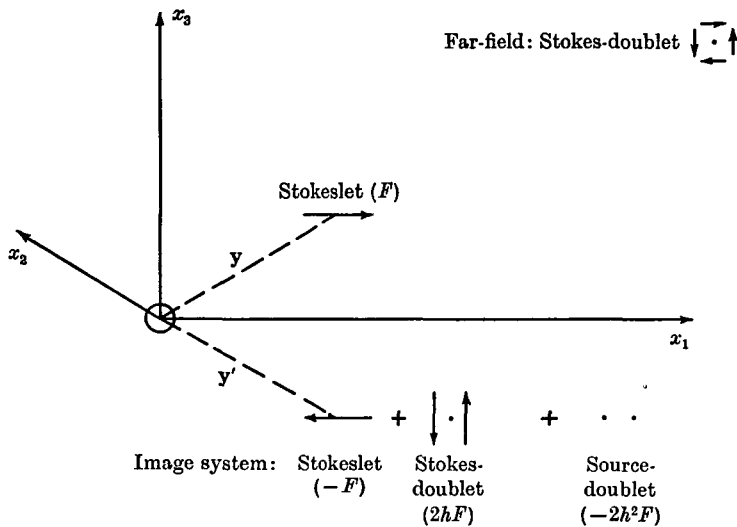


Fig. 3. Diagram illustrating image system for $k = 1$, the strength of the components being given in brackets.

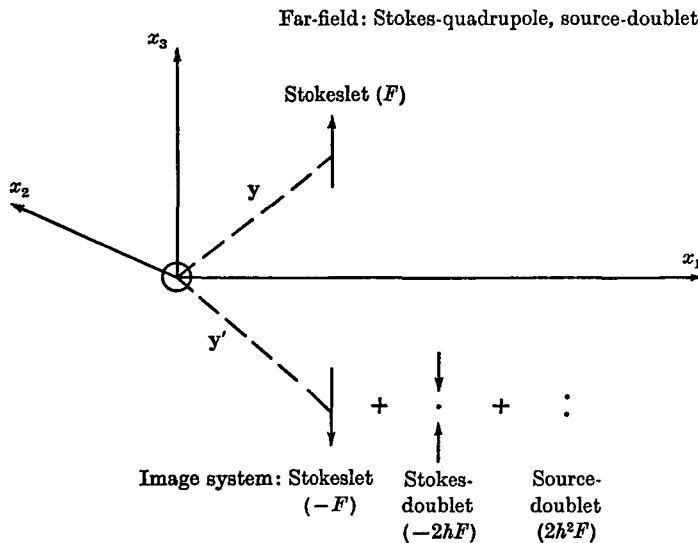


Fig. 4. Diagram illustrating image system for $k = 3$, the strength of the components being given in brackets.

The alternative orientation for the initial stokeslet is in the normal direction to the wall. The image system again consists of a negative stokeslet of equal magnitude, but this time the other complementary terms in the stokes-doublet and the source-doublet have a change in sign from the previous case of an initial stokeslet parallel to the wall. The stokes-doublet in this case consists of two stokeslets equal in magnitude, opposite in sign, orientated in the normal (x_3) direction, with displacement axis in the x_3 -direction, which is represented by $-D_{33}$. However, in this case, the velocity field is axisymmetric about the stokeslets, so that the image stokes-doublet consists only of a stresslet. The two diagrams of these above cases further emphasize these comments.

4. *Far-field effects.* In the far-field, the two stokeslets act as a stokes-doublet with their displacement axis in the x_3 -direction (i.e. tensor character D_{j3}). Thus we have to consider the effects of the two stokes-doublets of equal magnitude separated by a distance h . In the case of the initial stokeslet parallel to the wall, both effective stokes-doublets (i.e. D_{13} and D_{31}) are of the same sign, so that the far-field is that of a stokes-doublet of strength $4hF_1$ at $\frac{1}{2}(\mathbf{y} + \mathbf{y}')$. This far-field effect is of stresslet character, as the anti-symmetric terms due to the two stokes-doublets cancel, thus leaving only the symmetric stresslet terms. However, in the case of the initial stokeslet normal to the wall, the two stokes-doublets (both D_{33}) are opposite in sign, hence cancelling each others, doublet effect and therefore giving rise to a stokes-quadrupole velocity field in the far-field of magnitude $2h^2F$. This quadrupole field is of the same order of magnitude ($O(r^{-3})$) as that due to the source-doublet, so that the far-field will be a combination of a stokes-quadrupole and a source-doublet velocity field (strength $2h^2F$). Thus, there is a fundamental difference in the far-field velocity fields due to a point force acting parallel to a plane boundary than that due to a point force acting normal to the boundary.

To give us further insight into the influence of the stokeslets and image system, we can consider the equilibration of the force and couple over a hemisphere of fluid. The following surface integrals for the force and couple are used. As these integrals are the same for any surface enclosing the point force we choose the hemisphere of large radius a and the plane boundary ($x_3 = 0$). Thus

$$F_k = -\lim_{a \rightarrow \infty} \int_{A_1 + A_2} \sigma_{kj} n_j dA \quad (18)$$

$$\text{and} \quad L_i = \lim_{a \rightarrow \infty} \int_{A_1 + A_2} \epsilon_{ijk} x_j \sigma_{ki} n_i dA, \quad (19)$$

$$\left. \begin{aligned} \text{where} \quad \sigma_{kj} &= -p^* \delta_{kj} + \mu \left(\frac{\partial u_k^*}{\partial x_j} + \frac{\partial u_j^*}{\partial x_k} \right), \\ A_1 &= \{(x_1, x_2, x_3) | x_1^2 + x_2^2 \leq a^2; x_3 = 0\}, \\ A_2 &= \{(x_1, x_2, x_3) | x_1^2 + x_2^2 + x_3^2 = a^2; x_3 \geq 0\}, \end{aligned} \right\} \quad (20)$$

and \mathbf{n} is the outward normal to these surfaces. It is found that on the hemisphere of

large radius (i.e. A_2) there is no contribution to the force and couple integrals. The couple integral from A_1 is,

$$L_i = h(\delta_{i1}F_2 + \delta_{i2}F_1) \quad (21)$$

whereas the force integral is naturally equal to F_k on the plane boundary.

In conclusion, this paper gives us a better interpretation of the velocity and pressure fields due to a point force in the presence of a plane boundary, and the effects upon the far-field. It will be seen in later work how this allows us to understand the movement of slender bodies (e.g. micro-organisms) in the vicinity of walls.

This research was carried out while the author was in receipt of a George Murray Scholarship from the University of Adelaide, and a studentship from C.S.I.R.O. of Australia. Comments and suggestions from Professor M. J. Lighthill are acknowledged.

REFERENCES

- (1) BATCHELOR, G. K. *J. Fluid Mech.* **41** (1970), 545.
- (2) COX, R. G. *J. Fluid Mech.* **44** (1970), 791.
- (3) HAPPEL, J. and BRENNER, H. *Low Reynolds Number Hydrodynamics* (Prentice-Hall; Englewood Cliffs, N.J. 1965).
- (4) EJIKE, V. B. C. O. *Internat. J. Engng. Sci.* **8** (1970), 891.
- (5) ERDELYI, A. *Table of Integral Transforms* (McGraw-Hill; New York, 1954).
- (6) LADYZHENSKAYA, O. A. *The mathematical theory of viscous incompressible flow* (Gordon and Breach; London 1963).
- (7) LORENTZ, H. A. *Zittingsverlag Akad. v. Wet.* **5** (1896), 168.
- (8) SNEDDON, I. N. *Fourier Transforms* (McGraw-Hill; New York, 1951).
- (9) STOKES, G. G. *Trans. Cambridge Philos. Soc.* **9** (1851), 8.